Localization and AoA Estimation in 5G/6G

Dhanesh Kumar
Department of ECE
Indian Institute of Science
Bengaluru, India
dhaneshkumar@iisc.ac.in

Bharadwaj Amrutur
Department of ECE
Indian Institute of Science
Bengaluru, India
amrutur@iisc.ac.in

***Abstract*—This report introduces a novel 5G/6G-enabled framework for Simultaneous Localization and Mapping (SLAM) in dynamic construction environments, combining trilateration and MUltiple SIgnal Classification (MUSIC) algorithms to achieve real-time robot positioning and orientation. A robot equipped with a 5G receiver estimates its location using time-of-flight-derived ranges from 3–4 base stations and refines orientation via MUSIC-based Angle of Arrival (AoA) estimation applied to Channel State Information (CSI). Validation involved simulating a digital twin of IISc's ECE Department in the Sionna ray-tracing platform to model multipath propagation, followed by hardware deployment using an 8×8 antenna array setup (Tx/Rx) with Software-Defined Radios (USRP X310) and Python/MATLAB-based post-processing.**

***Index Terms*—Integrated Sensing and Communication(ISAC), Dataset, 6G-mmWave, Sionna, Ray Tracing**

I. Introduction

The convergence of sensing and communication in emerging 6G networks, known as Integrated Sensing and Communication (ISAC), is revolutionizing robotic perception systems, particularly for **Simultaneous Localization and Mapping (SLAM)** in dynamic environments such as construction sites. Traditional SLAM approaches, which rely primarily on LiDAR or camera arrays, often struggle in industrial settings due to occlusions, dust, and low-light conditions—challenges that are prevalent in construction and manufacturing domains.

This work presents a 5G/6G-enabled SLAM framework that leverages cellular infrastructure as both a communication backbone and a distributed sensing network, addressing these limitations through multimodal RF-vision fusion. Modern 5G systems utilize wideband millimeter-wave (mmWave) signals and massive MIMO antenna arrays, enabling high-precision positioning through time-of-flight (ToF) measurements and subspace-based Angle-of-Arrival (AoA) estimation using the MUSIC algorithm. Unlike conventional Received Signal Strength Indicator (RSSI)-based localization, our approach combines: (1) trilateration using three or four base stations for coarse positioning; (2) AoA refinement via Channel State Information (CSI) analysis; and (3) digital twin-assisted ray tracing using the Sionna platform to handle multipath propagation in complex, cluttered environments.

The proposed framework is validated through simulation, with hardware data collection completed for future validation. A digital twin of the IISc ECE department was modeled and simulated in Sionna for realistic propagation analysis, where trilateration and MUSIC algorithms were applied to synthetic data. The hardware testbed employs 8×8 antenna arrays and software-defined radios (USRP X310) to collect real-world measurements, with processing and validation against synthetic results planned for future work. This pipeline highlights three key advantages over traditional SLAM:

(i) *infrastructure reuse*, as existing 5G/6G base stations serve dual roles in communication and sensing.

(ii) *all-weather reliability*, since mmWave signals are less affected by visual obstructions.

(iii) *scalability*, enabling large-area mapping through centralized fusion of distributed measurements.

This work aligns with the 3GPP ISAC roadmap for 6G networks [1], demonstrating how communication signals can be repurposed for robotic navigation in challenging environments. The integrated simulation-hardware pipeline bridges the gap between theoretical ISAC concepts and deployable industrial SLAM solutions.

In the 5G-A and 6G era, ISAC technology is anticipated to be used in various intelligent applications that demand a high data transmission rate and precise sensing capabilities. We believe in 6G the mobile network will cleverly connect smart devices with a lot of intelligence. These intelligent nodes can sense their environment and communicate back and forth with one another about what they observe. Networked sensing will be a characteristic of 6G.

The remainder of this report is organized as follows:
Section II provides an overview of Integrated Sensing & Communication (ISAC) and Simultaneous Localization and Mapping (SLAM), structured into three parts: Part A covers the fundamentals of ISAC, Part B is about SLAM and part C covers the various use cases of RF Sensing in SLAM. Section III outlines the motivation and problem statement of this work, while the proposed approach & Preliminary results are presented in Section IV, and the conclusion & future scope of the project is discussed in the later Section.

II. Integrated Sensing & Communication and SLAM

A. Integrated Sensing & Communication(ISAC):

Radar systems and communication systems share several common modules, fostering synergy between these two technological domains. Both systems utilize similar antenna systems for signal transmission and reception, emphasizing com-

mon principles in antenna design and beamforming techniques. Both systems employ complex techniques for modulation, demodulation, and the extraction of relevant information from received signals. Bringing these processes together not only makes the hardware simpler but also allows us to create integrated systems that can handle sensing and communication tasks well. This integration makes the overall system work better and be more adaptable to different needs.

B. Simultaneous Localization and Mapping (SLAM):

Simultaneous Localization and Mapping (SLAM) is a computational framework that enables autonomous systems—such as robots, drones, and self-driving vehicles—to navigate and map unfamiliar environments while simultaneously determining their own position within those environments. SLAM algorithms fuse data from various sensors, including cameras, LiDAR, sonar, and inertial measurement units (IMUs), to build a map of the surroundings and estimate the robot's pose (position and orientation) in real time. This dual capability allows robots to operate effectively even in environments where prior maps do not exist.

C. RF-Based Sensing in SLAM:

Radio Frequency (RF) sensing enables Simultaneous Localization and Mapping (SLAM) by leveraging electromagnetic waves for spatial awareness in environments where traditional sensors (e.g., LiDAR, cameras) face limitations. This approach utilizes signal properties like Time-of-Flight (ToF), Angle-of-Arrival (AoA), and Channel State Information (CSI) to resolve positional uncertainty and construct environmental maps [2], [3].

1) Enhanced Navigation in Challenging Environments:
Indoor Navigation: RF-SLAM overcomes poor lighting and featureless spaces using existing RF infrastructure (e.g., WiFi access points, RFID tags). Warehouse robots demonstrate decimeter-level accuracy by fusing RF measurements with inertial data [4], [5].

Dynamic Environments: RF signals penetrate smoke, dust, and moving obstacles, maintaining functionality where visual sensors fail. UWB radar achieves centimeter-level accuracy in cluttered industrial settings by waveform matching [6].

Featureless Spaces: In GPS-denied areas like tunnels, RFID-based topological mapping creates navigable graphs using tag clusters as landmarks [7].

2) Warehouse Automation and Logistics:

- **Automated Guided Vehicles (AGVs):** RF-SLAM enables centimeter-accurate path planning using UHF-RFID tags for real-time inventory localization [2].
- **Robotic Picking:** RFID-tagged items allow robots to locate products 34% faster than vision-based systems in high-shelf warehouses [4].
- **Inventory Management:** Continuous radio map updates using 5G UMa propagation models enable live inventory tracking without manual calibration [5].

3) Specialized Applications:

- **Search and Rescue:** Multi-robot RF-SLAM systems collaboratively map disaster zones using tree features as stable landmarks, improving loop closure recall by 40% in occluded environments [7].
- **Construction/Mining:** 5G NR signals enable 3D mapping of dynamic sites using MUSIC-based AoA estimation, with digital twins validating multipath effects [2].
- **Healthcare:** UWB-based asset tracking locates medical equipment with ¡10 cm error in EMI-rich hospital environments [4].

TABLE I: RF-SLAM Methodologies Summary

Method	**Characteristics**	
	Key Features	***Applications***
RFID-based	Sparse tag deployment, low-cost	Warehouse inventory, planogram compliance [4]
WiFi-based	Uses existing infrastructure, 26.9cm median accuracy	Indoor navigation, large-area mapping [6]
UWB-based	Sub-0.5m accuracy, smoke/NLOS resistant	Search and rescue, construction sites [7]
Hybrid	Combines RF with vision/LiDAR for drift correction	Autonomous vehicles, dynamic environments [3]

RF-SLAM provides a versatile solution for robotic navigation in visually degraded environments, transforming communication signals into spatial awareness capabilities.

III. Motivation & Problem Statement

Current SLAM systems primarily rely on vision-based sensors such as LiDAR and cameras for localization and mapping tasks. While effective in many scenarios, these technologies often fail in environments with dust, smoke, poor lighting, or frequent occlusions—conditions common in construction sites and other challenging settings. In contrast, radio frequency (RF) signals, particularly at 28 GHz, offer significant advantages due to their ability to penetrate visual obstructions and provide robust multipath information. Despite this potential, there is a lack of high-quality datasets and research focused on leveraging 28 GHz RF signals for SLAM. This work is motivated by the need to address these limitations and to explore the integration of high-frequency RF sensing into SLAM frameworks, aiming to enable reliable robotic navigation where traditional vision-based systems are inadequate.

IV. Proposed Approach and Data Collection

A. Hardware Setup

For data collection, we utilized a mmWave base station at the Bharat 5G Lab, ARTPARK, IISc, Bengaluru. The setup architecture is based on a 5G FR2 communication system and consists of the following components:

- **Up/Down Converter Box (UDB) Single Band 5G:** The UDB-S-G from TMYTEK is a versatile up/down frequency converter, supporting RF frequencies from 24 to 44 GHz and featuring a built-in local oscillator for seamless integration. It enables efficient frequency conversion between mmWave and IF bands, making it ideal

for extending the capabilities of existing sub-6 GHz test equipment into the 5G and 6G mmWave range. [8], [9]

- **BBox One 5G 28 GHz (Beamformer):** BBox One 5G 28GHz from TMYTEK is a compact, ready-to-use mmWave beamforming development tool designed for 5G New Radio (NR) applications, particularly in the 28 GHz band (operating frequency: 26.5–29.5 GHz, covering 5G n257 band). It features up to 16 individually controllable RF channels, each with 360° phase shifter coverage (5° step), 15 dB attenuation range (0.5 dB step), and supports 2D beamforming and steering with 8x8 antenna array. The device integrates key RF components (T/R switch, LNA/PA, phase shifters) and provides software control via Ethernet or SPI interface, enabling precise phase and amplitude adjustments for advanced 5G beam steering and MIMO research. [8], [9]
- **USRP X310:** The USRP X310 is a high-performance, scalable software-defined radio (SDR) platform, designed for advanced wireless prototyping and research. The USRP X310 can be integrated with external up/down converters to extend its frequency coverage. In this configuration, the USRP generates or receives intermediate frequency (IF) signals, which are converted to or from higher RF frequencies by the up/down converter, enabling operation in frequency bands beyond the X310's native range. It is compatible with open-source UHD software, GNU Radio.
- **A Laptop/Desktop:** The control setup requires a laptop running **TMXLAB Kit** for hardware control and **GNU Radio** for signal processing. TMXLAB Kit configures the UD Box's frequency conversion (e.g., 27 GHz RF $\leftrightarrow$ 429 MHz IF) and the BBox One's beam parameters (phase/amplitude per RF channel) [8], [9]. The TMYTEK interface is shown in `Fig.15`, 16.GNU Radio handles baseband waveform generation/acquisition via the USRP X310 [10].

TABLE II: Software Functions

Software	Role
TMXLAB Kit	UD Box LO control, BBox beam steering
GNU Radio	Baseband signal processing

B. Data Collection

Fig. 1: Hardware Setup

- **mmWave RF Data:** The data collected before transmission and after modulation at the Transmitter end, and at the receiver end it is collected after demodulation in the raw format. The raw data is initially stored in `.dat` format, which is then converted to `.mat` format during post-processing. The processed data, structured as an $N \times M$ matrix—where N represents the number of subcarriers (SC) in each symbol and M represents the number of symbols in the radio frame—is stored in `.mat` format for further analysis. The Block Diagram of OFDM simulations using USRP X310 in the GNU radio Companion software is shown in the `Fig.2`(for Transmitter) and `Fig.3`(for Receiver).

The hardware setup for data collection is illustrated in `Fig.1` and the parameter used for the dataset generation is given in `Table` III.

TABLE III

Parameters	Value
Number of Symbols	1120
Antenna array size	8x8
FFT Size	8192
CP Length	256
Carrier Frequency	27.429 GHz
Sampling rate	1M

C. Dataset Description

1) RF Data: The RF dataset curated for this study adheres to 5G communication standards and provides a comprehensive and diverse collection of synchronized radio frequency (RF). This dataset is essential for advancing research in integrated sensing and communication (ISAC). The data collected for the Receiver at 6 different positions i.e., {0.25, 0.5, 0.75, 1, 1.5, 2}metre distance from the Transmitter, to study RF responses under different static conditions.

2) Signal Analysis Results: Four plots are presented (ref. to `Fig.4`), corresponding to the experiment at 1 metre:

Plot	Description
Tx Spectrum	Shows the transmitted OFDM signal spectrum, which is flat across the occupied bandwidth, indicating proper signal generation and spectral containment.
Rx Spectrum	Displays the received signal spectrum centered at 429.307 MHz (IF), with a relative gain of -124 dB, confirming successful signal recovery and low noise.
Rx Constellation	Scatter plot of the received symbols before demodulation, showing some dispersion due to channel noise and multipath.
Demod Constellation	Scatter plot after QPSK demodulation, with visible clustering at the four QPSK constellation points, indicating almost accurate demodulation and minimal distortion.

TABLE IV: Signal analysis results for hardware setup at 1 metre distance

These results validate the effectiveness of the hardware setup for robust mmWave signal transmission and reception at short range. The spectral and constellation plots demonstrate that the system maintains good signal integrity, and the

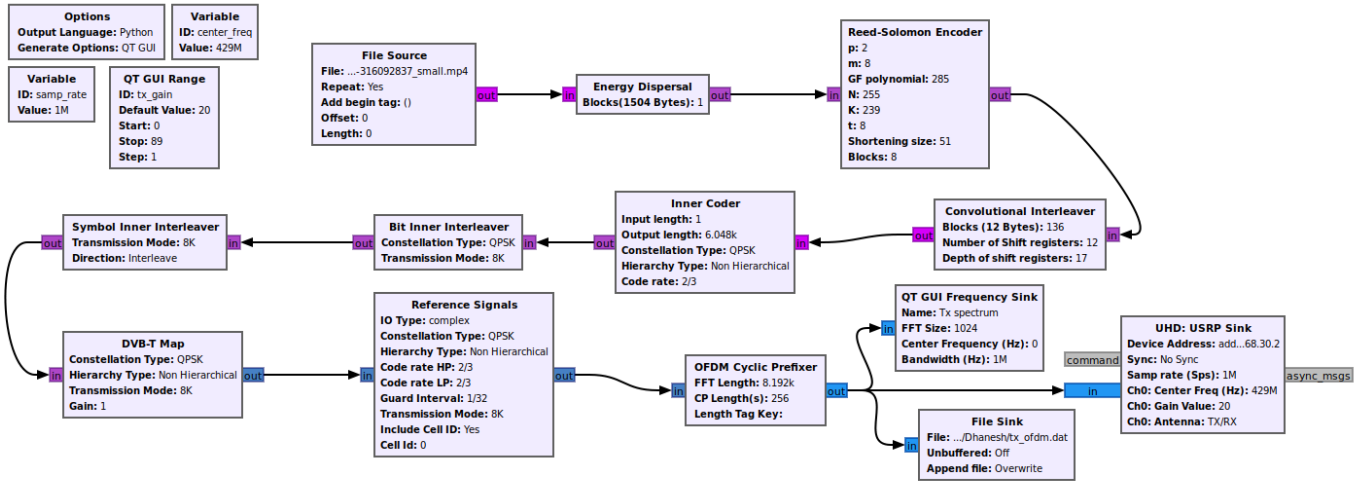

Fig. 2: OFDM Simulations in GNU radio Companion (Transmitter)

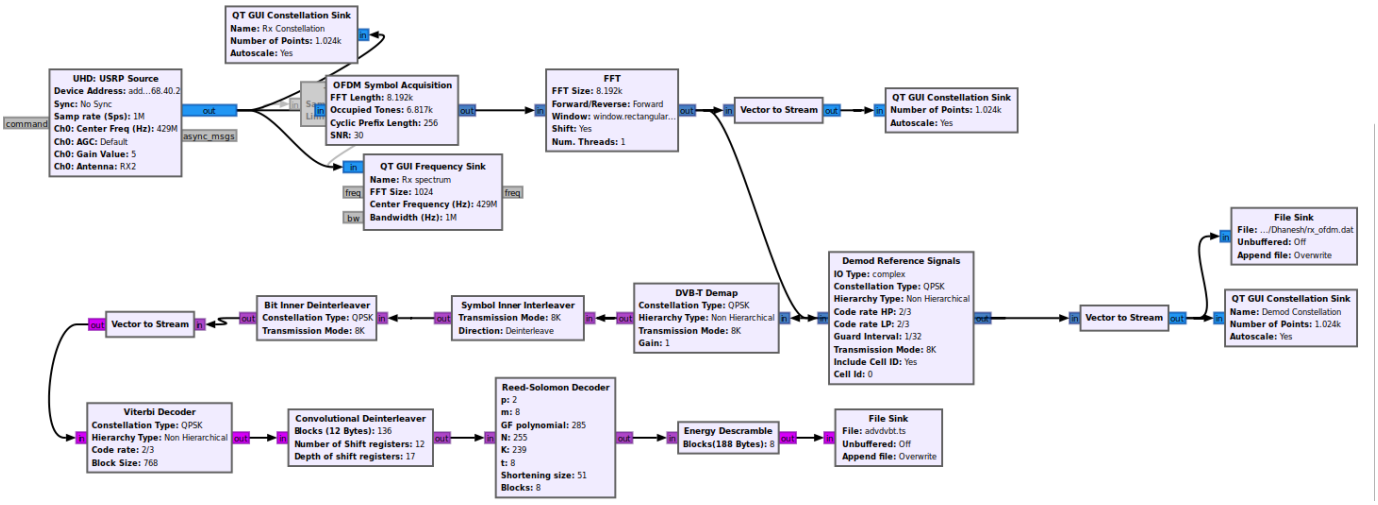

Fig. 3: OFDM Simulations in GNU radio Companion (Receiver)

demodulated output confirms the feasibility of using this setup for high-precision localization and sensing applications.

D. Synthetic Data Generation and Simulation Results

The architecture for generating synthetic dataset using Sionna-RT [11] is given in the `Fig.5` and the parameters for the used propagation model is in `Table` V.

TABLE V

Parameters	Value
Number of OFDM Symbols	1024
FFT Size	1024
Number of Transmitter	3
Transmitter array size	8x4
Number of Receiver	1
Receiver array size	4x4
Subcarrier Spacing	30KHz
Carrier Frequency	3.5 GHz

1) Scene Creation: We use Blender tools to replicate a real-world indoor environment digitally. This digital *scene* undergoes meticulous importation into Sionna RT from Blender employing `Mitsuba 3`, facilitating precise `.xml` format utilization. Sionna categorizes all scene components as *radio materials* for accurate calculations and *radio properties*.

2) Propagation Modeling using Sionna-RT: Following scene creation, the propagation modeling process in Sionna RT begins by integrating Sionna with the LLVM toolchain for seamless compatibility. This integration ensures the systematic inclusion of receivers and transmitters, replicating real-world scenarios within the scene. Computational algorithms compute signal paths, generating comprehensive coverage maps visualizing signal propagation patterns. `Fig.6` displays a sample of the generated propagation model.

3) Post-processing:

- Localization: Upon obtaining the channel state information (CSI) data from Sionna-RT, the data is initially transformed from the time-frequency domain to the delay-Doppler domain using the Symplectic Finite Fourier Transform (SFFT). This transformation enables accurate estimation of the range between each transmitter and receiver. The detailed algorithm and corresponding for-

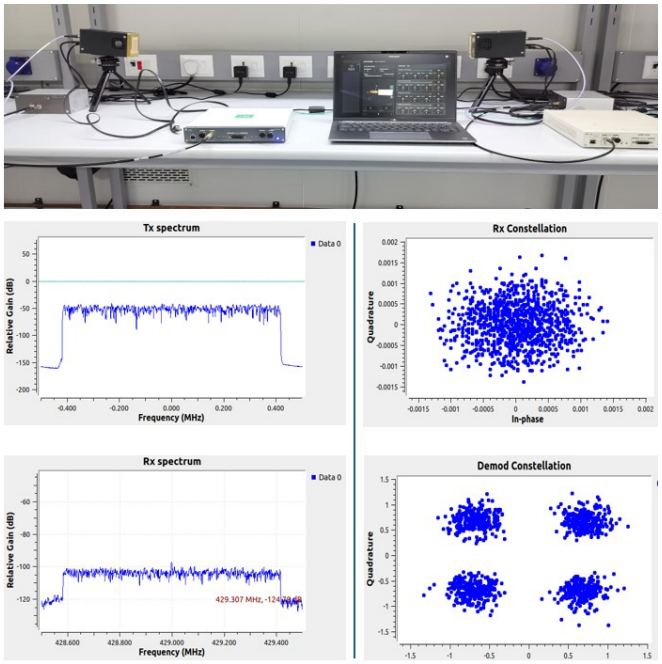

Fig. 4: Hardware setup at 1 metre and its simulation result

mulae for applying the SFFT to the CSI data are provided in the **Appendix** B. Subsequently, the estimated ranges are utilized as inputs to a trilateration algorithm (refer **Appendix** C), which determines the precise location of the receiver within the environment.

- Angle of Arrival estimation: Following range estimation, the Angle of Arrival (AoA) is determined by applying the Multiple Signal Classification (MUSIC) algorithm [12] to the Channel State Information (CSI) data. MUSIC is a high-resolution subspace-based algorithm that leverages the eigenstructure of the spatial covariance matrix to estimate signal directions.

In `Fig.8` it is shown a bigger picture of AoA estimation using MUSIC Algorithm.

The algorithm for AoA estimation proceeds as follows:

1) Construct the spatial covariance matrix $\mathbf{R}$ from the CSI data:
$$\mathbf{R} = \frac{1}{N}\sum_{n=1}^{N} \mathbf{H}(n)\mathbf{H}^H(n)$$
where $\mathbf{H}(n)$ is the CSI matrix for the n-th subcarrier and N is the total number of subcarriers.
2) Perform eigenvalue decomposition of $\mathbf{R}$:
$$\mathbf{R} = \mathbf{E}_s\mathbf{\Lambda}_s\mathbf{E}_s^H + \mathbf{E}_n\mathbf{\Lambda}_n\mathbf{E}_n^H$$
where $\mathbf{E}_s$ contains signal subspace eigenvectors and $\mathbf{E}_n$ contains noise subspace eigenvectors.
3) Compute the MUSIC spatial spectrum:
$$P(\theta) = \frac{1}{\mathbf{a}^H(\theta)\mathbf{E}_n\mathbf{E}_n^H\mathbf{a}(\theta)}$$
where $\mathbf{a}(\theta)$ is the steering vector corresponding to angle θ.
4) Identify AoA as the peaks in $P(\theta)$.

The MUSIC algorithm provides superior angular resolution compared to conventional beamforming techniques, enabling precise localization when combined with range estimates from the delay-Doppler domain transformation.

4) Results: The results of simulation on synthetic data for localization and AoA estimation are summarized in `Table` VI. Using the Sionna-RT platform, a digital twin of the IISc ECE Department was created with three transmitters and one receiver. The receiver's position was estimated using trilateration based on range measurements, and the Angle of Arrival (AoA) was determined using the MUSIC algorithm applied to channel state information.

CONCLUSION AND FUTURE SCOPE

This project developed and validated a 5G/6G-enabled SLAM framework tailored for robotic navigation in dynamic construction environments, focusing on mmWave signals at 28 GHz. The dataset collected contains 28 GHz RF measurements, providing a foundation for advanced localization techniques. While the current dataset supports single-point measurements, future implementation of trilateration for precise positioning will require deployment of two or three additional transmitter devices to provide sufficient geometric diversity. Similarly, application of the MUSIC algorithm for high-resolution Angle of Arrival (AoA) estimation will be enabled once multiple transmitters are available, permitting joint range and direction estimation from Channel State Information (CSI).

Validation to date has been conducted through Sionna-based digital twin simulations, where trilateration and MUSIC algorithms were successfully applied to synthetic data. Hardware experiments utilizing 8×8 antenna arrays and the USRP N310 platform have collected initial RF measurements, with processing and validation against simulation results scheduled for future work. These preliminary results indicate the potential feasibility of leveraging 5G mmWave infrastructure for robust localization and mapping, particularly in environments where traditional vision-based SLAM systems face challenges due to occlusions, dust, or poor lighting. The integration of trilateration and MUSIC-based AoA estimation within this framework paves the way for future multi-anchor deployments and more accurate, real-time SLAM in complex industrial scenarios.

The dataset, simulation models, and implementation code are publicly available in the GitHub repository [13], enabling further research and development in RF-based SLAM systems.

ACKNOWLEDGMENT

First and foremost, I would like to express my deepest gratitude to my supervisor, **Prof. Bharadwaj Amrutur**, for his invaluable guidance, encouragement, and continuous support throughout the course of this project.

I am forever grateful to the Indian Institute of Science (IISc) for providing me with the opportunity to study and conduct research in cutting-edge technology.

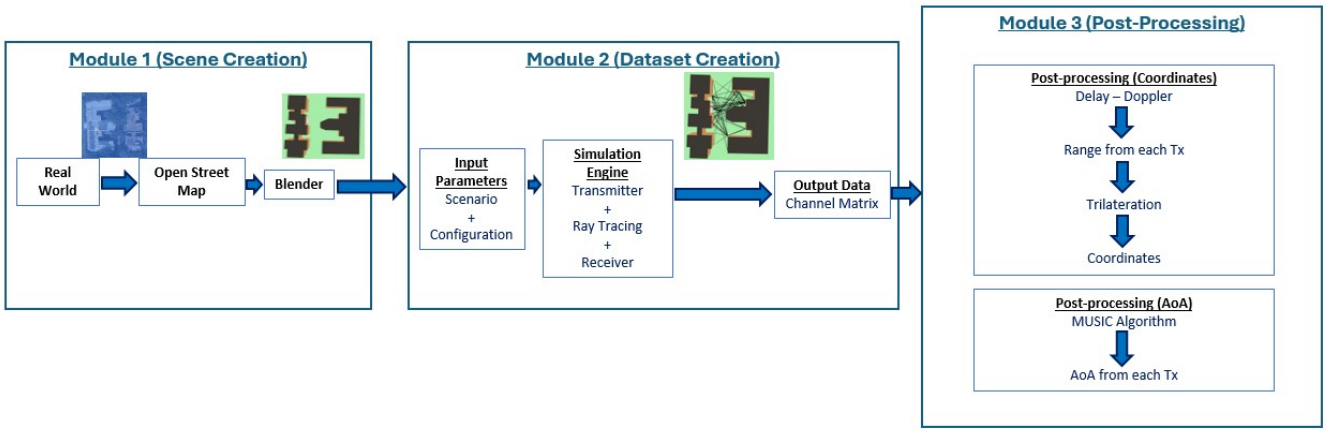

Fig. 5: Sionna-RT Simulation Architecture

TABLE VI: Localization and AoA Estimation Results using Synthetic Data

Scene	TX Locations	RX Location (original)	RX (est)	Error (LS)	AoA (org)	AoA (MUSIC)	Error (AoA)
IISc ECE Dept (6)	TX1: (12.8, 10.853,2.1) TX2: (-14.05, 17,2.1) TX3: (-2.5, -18.5,2.1)	(-8, 4,2.1)	(-8.39, 3.24,2.1)	0.8542 m	TX1: 18.236° TX2: 114.957° TX3: -76.264°	TX1: 17.681° TX2: 114.953° TX3: -55.338°	TX1: 0.555° TX2: 0.004° TX3: 20.926°
IISc ECE Dept (19)	TX1: (12.8, 10.853,2.1) TX2: (-14.05, 17,2.1) TX3: (-2.5, -18.5,2.1)	(-8, 15,2.1)	(-7.56, 16.12,2.1)	1.2033 m	TX1: -11.275° TX2: 161.707° TX3: -80.676°	TX1: -11.02° TX2: 161.67° TX3: -56.74°	TX1: 0.255° TX2: 0.037° TX3: 23.936°
Street Canyon (20)	TX1: (54, 10.3,2.1) TX2: (48, -8.55,2.1) TX3: (60, -8.55,2.1)	(2, 4,2.1)	(3.13, 3.67,2.1)	1.1772 m	TX1: 6.9079° TX2: -165.91° TX3: -12.21°	TX1: 7.21° TX2: -165.987° TX3: -8.07°	TX1: 0.3021° TX2: 0.04° TX3: 4.14°
Etiole (21)	TX1: (24, 38,2.1) TX2: (-78, 43,2.1) TX3: (-65,-56,2.1)	(-8, 4,2.1)	(-7.35, 4.729,2.1)	0.9767 m	TX1: 46.7357° TX2: 150.876° TX3: -133.53°	TX1: 46.643° TX2: 151.02° TX3: -100.91°	TX1: 0.0927° TX2: 0.144° TX3: 32.62°
Munich (22)	TX1: (0, 100,2.1) TX2: (40, 120,2.1) TX3: (80, 100,2.1)	(40, 50,2.1)	(36.61, 52.31,2.1)	4.1022 m	TX1: 128.6598° TX2: 90° TX3: 51.34°	TX1: 127.83° TX2: 90.61° TX3: 63.46°	TX1: 0.8298° TX2: 0.61° TX3: 12.06°

I would also like to thank **MeitY** for funding this project, and **Rathinamala Vijay** from ARTPARK for setting up the hardware at the ARTGarage, IISc and developing the modules in the GNU Radio Companion software for the hardware simulation.

Special thanks are due to my colleagues for their collaboration and assistance during this work.

Lastly, I would like to thank my family, especially my little sister, for their unwavering support and encouragement throughout my academic journey.

REFERENCES

[1] "Feasibility study on integrated sensing and communication (release 19)," Tech. Rep. 3GPP TR 22.837 V19.2.1, 3rd Generation Partnership Project (3GPP), Technical Specification Group SA, 02 2024. Available: https://www.3gpp.org/dynareport/22837.htm.

[2] P. T. Karfakis and P. T. Karfakis, "Nr5g-sam: A slam framework for field robot applications based on 5g new radio," *Journal Name*, 2023. PMCID: PMC10256012.

[3] A. Arun and W. e. a. Hunter, "Viwid: Leveraging wifi for robust and resource-efficient slam," *arXiv preprint arXiv:2209.08091*, 2022.

[4] B. Drake, *Implementation of Static RFID Landmarks in SLAM for Planogram Compliance*. PhD thesis, Georgia Southern University, 2023.

[5] M. J. Segura and F. A. A. Cheein, "Ultra wide-band localization and slam: A comparative study," *Journal Name*, 2011. PMCID: PMC3274006.

[6] A. Arun and R. Ayyalasomayajula, "P2slam: Bearing based wifi slam for indoor robots," *IEEE Robotics and Automation Letters*, 2021. DOI: 10.1109/LRA.2022.3144796.

[7] Y. Liu and Z. e. a. Jian, "Range-slam: Ultra-wideband-based smoke-resistant real-time localization and mapping," *arXiv preprint arXiv:2409.09763*, 2024.

[8] TMYTEK, "Bbox 5g — mmwave beamformer." https://tmytek.com/products/beamformers/bbox. Accessed: 2025-06-21.

[9] TMYTEK, *BBox One 5G 28 GHz Datasheet*, 2022.

[10] G. Radio, "Windowsinstall - gnu radio wiki," 2025. Available: https:

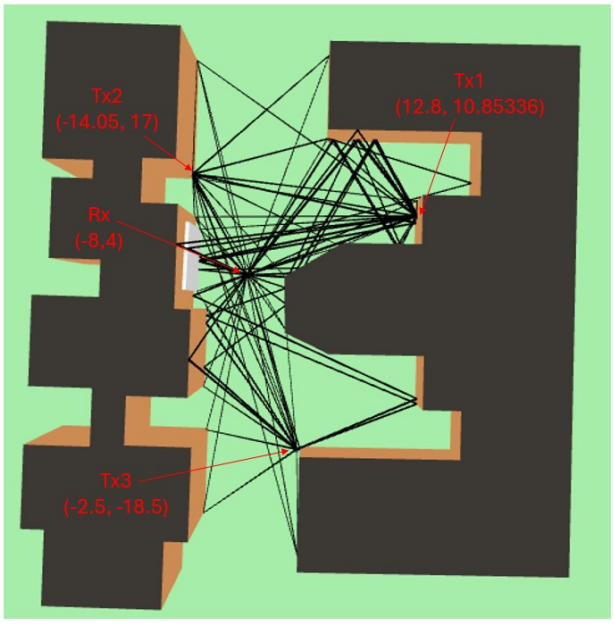

Fig. 6: Sionna-RT Example (ECE Dept., IISc)

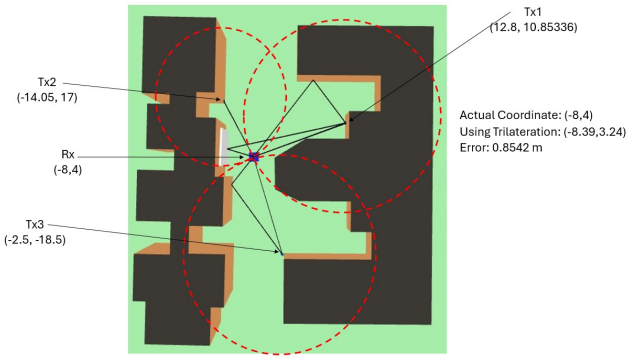

Fig. 7: 2D Localization using Trilateration

//wiki.gnuradio.org/index.php/WindowsInstall.

[11] J. Hoydis, F. Ait Aoudia, S. Cammerer, M. Nimier-David, N. Binder, G. Marcus, and A. Keller, "Sionna RT: Differentiable Ray Tracing for Radio Propagation Modeling," *arXiv preprint*, Mar. 2023.

[12] R. O. Schmidt, "Multiple emitter location and signal parameter estimation," *IEEE Transactions on Antennas and Propagation*, vol. 34, no. 3, pp. 276–280, 1986.

[13] D. Kumar, "Localization-and-aoa-estimation-in-5g-6g." https://github.com/kdhanesh327/Localization-and-AoA-estimation-in-5G-6G, 2025. GitHub repository.

[14] TMYTEK, *UD Box 5G Series Datasheet*, 2023. Available: https://www.tmytek.com/corpwebfiles/TMYTEK_DS_UD+Box+5G_GL.pdf.

[15] TMYTEK, "Tmxlab kit," 2023. Available: https://tmytek.com/resources/downloads/tmxlab-kit.

[16] M. Ubadah, S. K. Mohammed, R. Hadani, S. Kons, A. Chockalingam, and R. Calderbank, "Zak-otfs for integration of sensing and communication," 2024.

[17] M. Jafri, S. Srivastava, and A. K. Jagannatham, "Sparse target parameter and channel estimation in mmwave mimo otfs-aided integrated sensing and communication systems," 2023. M. Jafri is a Student Member, IEEE; S. Srivastava and A. K. Jagannatham are Members, IEEE.

[18] ScienceDirect Topics, "Trilateration - an overview — sciencedirect topics," 2024. Accessed: 2025-06-22.

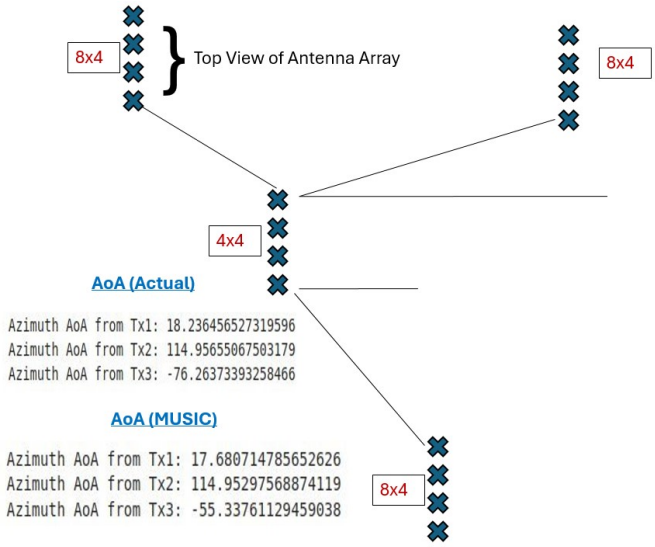

Fig. 8: AoA estimation using on Sionna-RT simulation data (Transmitter array size= 8x4 (17) and Receiver array size= 4x4 (18)

APPENDIX

A. Hardware Description:

1) Up/Down Converter Box (UDB) Single Band 5G [14]: The TMYTEK UD Box 5G is a broadband frequency converter designed for 5G mmWave research, development, and testing. It enables seamless integration between baseband processing equipment and mmWave systems by converting signals between intermediate frequency (IF) and radio frequency (RF) bands.

TABLE VII: Key Specifications of UD Box 5G [15]

Parameters	Value
RF Range	24–44 GHz
IF Range	0.01–14 GHz
LO Range	24–44 GHz (1 Hz resolution)
Conversion Loss	12–13 dB (typical)
Phase Noise	< -100 dBc/Hz @ 1 MHz offset
Control Interface	Ethernet (RJ-45)
Reference Input	10 MHz, 100 MHz
Power Supply	12 V DC
Dimensions	200 × 120 × 40 mm

(a) (b)

Fig. 9: Up/Down Converter Box (UDB) Single Band 5G: (a) Front Panel, (b) Back Panel

2) BBox One 5G 28 GHz (Beamformer) [8]: The **BBox One 5G 28 GHz** is a compact, programmable mmWave beamforming development tool designed for 5G NR research and prototyping, specifically targeting the n257 band (26.5–29.5 GHz). It features 16 independent RF channels, each with precise phase (360°, 5° steps) and amplitude (15 dB range, 0.5 dB steps) control, enabling advanced beam steering and shaping. The system supports half-duplex operation, integrating transmit/receive (T/R) switches, power amplifiers, low-noise amplifiers, and phase shifters. Control is provided via a GUI or API over Ethernet or SPI, allowing real-time beam management and easy integration with SDR platforms. It is suitable for MIMO, beam tracking, and 5G protocol development in both laboratory and advanced wireless system environments. It uses a grouping technique to connect its 16 RF channels to an 8x8 antenna array (64 elements). Every four antenna elements share one RF channel, forming a sub-array. Since 64 ÷ 4 = 16, this matches the 16 available channels.

TABLE VIII: Key Parameters of BBox One 5G 28 GHz Beamformer [9]

Parameter	Value
Frequency Range	26.5–29.5 GHz (n257 band)
Number of Channels	16 RF channels
Phase Control	0–360° (5° steps)
Amplitude Control	0–15 dB (0.5 dB steps)
Operation Mode	Half-duplex (T/R switch)
Control Interface	Ethernet (RJ-45), SPI
Beam Steering Speed	2 μs (via SPI)
Antenna Array	Detachable standard array or custom
Dimensions	156 × 82 × 82 mm

Fig. 10: BBox One 5G 28 GHz Beamformer

B. Range Calculation from CSI Data

Time-Frequency to Delay-Doppler Domain Conversion [16], [17]: **Definitions:**

- N: Number of subcarriers (frequency bins)
- M: Number of symbols (time slots)
- n: Time index ($n = 0, 1, \ldots, M-1$)
- m: Subcarrier index ($m = 0, 1, \ldots, N-1$)
- k: Delay index ($k = 0, 1, \ldots, N-1$)
- l: Doppler index ($l = 0, 1, \ldots, M-1$)

Input:

- Time-frequency domain CSI matrix $H_{\mathrm{TF}}[n, m]$ of size $M \times N$

Output:

- Delay-Doppler domain CSI matrix $H_{\mathrm{DD}}[k, l]$ of size $N \times M$

Algorithm 1 TF to DD Domain Conversion

Initialize: $H_{\mathrm{DD}} \leftarrow \mathrm{zeros}(N, M)$
for $k = 0$ to $N-1$ **do**
  {Delay index} **for** $l = 0$ to $M-1$ **do** {Doppler index}
    $sum \leftarrow 0$
    for $n = 0$ to $M-1$ **do**
      {Time index} **for** $m = 0$ to $N-1$ **do** {Subcarrier index}
      $\phi \leftarrow -j2\pi \left(\frac{nl}{M} - \frac{mk}{N}\right)$
      $sum \leftarrow sum + H_{\mathrm{TF}}[n, m] \cdot \exp(\phi)$
    end for
    end for
    $H_{\mathrm{DD}}[k, l] \leftarrow \frac{sum}{\sqrt{MN}}$
  end for
end for
Return H_{DD}

Conversion Formula:

$$H_{\mathrm{DD}}[k,l] = \frac{1}{\sqrt{MN}} \sum_{n=0}^{M-1} \sum_{m=0}^{N-1} H_{\mathrm{TF}}[n,m] \cdot \exp\left(-j2\pi\left(\frac{nl}{M} - \frac{mk}{N}\right)\right) \quad (1)$$

Algorithm 2 Peak Detection from CSI in Delay-Doppler Domain

Require: Delay-Doppler CSI matrix $\mathbf{H}_{dd} \in \mathbb{C}^{N \times M}$
Ensure: Indices $(k_{\max}, l_{\max})$ and value $P_{\max}$ of the maximum peak
Compute power profile: $\mathbf{P} = |\mathbf{H}_{dd}|^2$
Find maximum value: $P_{\max} = \max(\mathbf{P})$
Find indices of maximum: $(k_{\max}, l_{\max}) = \mathrm{argmax}_{k,l}\, \mathbf{P}[k, l]$
return $(k_{\max}, l_{\max}, P_{\max})$

Algorithm 3 Range Calculation from Peak Detection

Require: Delay index $k_{\max}$ from peak detection
Require: Speed of light $c = 3 \times 10^8$ m/s
Require: Subcarrier spacing Δf (Hz)
Require: Number of delay bins N
Require: Path type flag: $isLOS$ (boolean)
Ensure: Range estimate R
Calculate delay in seconds: $\tau = \frac{k_{\max}}{N \cdot \Delta f}$
if $isLOS$ **then**
  $R = \tau \cdot c$ {Line-of-Sight calculation}
else
  $R = \tau \cdot c/2$ {Non-Line-of-Sight calculation}
end if
return R

C. 2D Trilateration [18]

Definitions:

- Transmitters: $T_1 = (x_1, y_1), T_2 = (x_2, y_2), T_3 = (x_3, y_3)$
- Receiver: Unknown position $R = (x, y)$
- Measured distances: d_1 (to T_1), d_2 (to T_2), d_3 (to T_3)

Definitions:

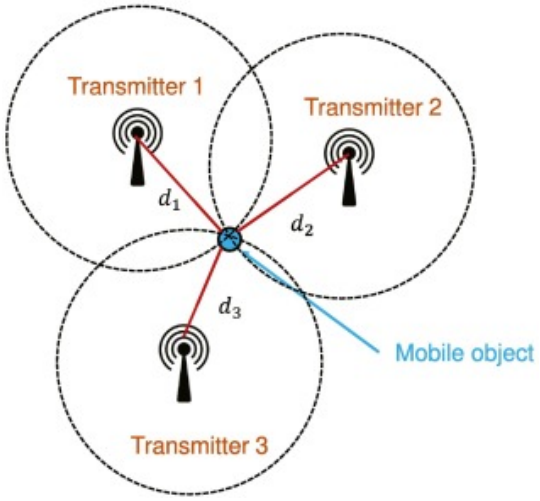

Fig. 11: Trilateration using 3 Transmitter and 1 UE [18]

Step 1: Circle Equations

$$(x - x_1)^2 + (y - y_1)^2 = d_1^2 \tag{2}$$
$$(x - x_2)^2 + (y - y_2)^2 = d_2^2 \tag{3}$$
$$(x - x_3)^2 + (y - y_3)^2 = d_3^2 \tag{4}$$

Step 2: Linearization (Subtract (2) from (3) and (4))

$$2(x_2 - x_1)x + 2(y_2 - y_1)y = d_1^2 - d_2^2 - x_1^2 + x_2^2 - y_1^2 + y_2^2$$
$$2(x_3 - x_1)x + 2(y_3 - y_1)y = d_1^2 - d_3^2 - x_1^2 + x_3^2 - y_1^2 + y_3^2$$

Step 3: Matrix Form

$$\begin{bmatrix} 2(x_2 - x_1) & 2(y_2 - y_1) \\ 2(x_3 - x_1) & 2(y_3 - y_1) \end{bmatrix} \begin{bmatrix} x \\ y \end{bmatrix} = \begin{bmatrix} C_1 \\ C_2 \end{bmatrix}$$

where

$$C_1 = d_1^2 - d_2^2 - x_1^2 + x_2^2 - y_1^2 + y_2^2$$
$$C_2 = d_1^2 - d_3^2 - x_1^2 + x_3^2 - y_1^2 + y_3^2$$

Step 4: Solution

$$\begin{bmatrix} x \\ y \end{bmatrix} = \frac{1}{\det A} \begin{bmatrix} A_{22} & -A_{12} \\ -A_{21} & A_{11} \end{bmatrix} \begin{bmatrix} C_1 \\ C_2 \end{bmatrix}$$

where A_{ij} are the elements of the coefficient matrix A and $\det A = A_{11}A_{22} - A_{12}A_{21}$.

D. Miscellaneous

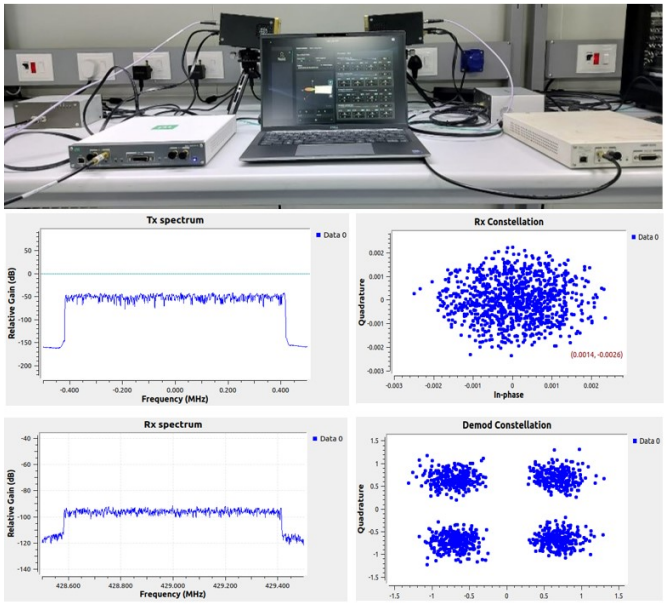

Fig. 12: Hardware setup at 0.25 metre and its simulation result

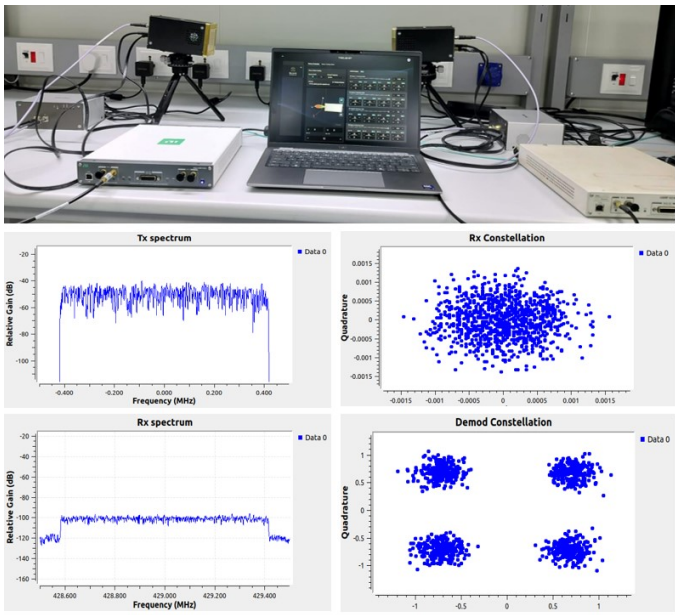

Fig. 13: Hardware setup at 0.5 metre and its simulation result

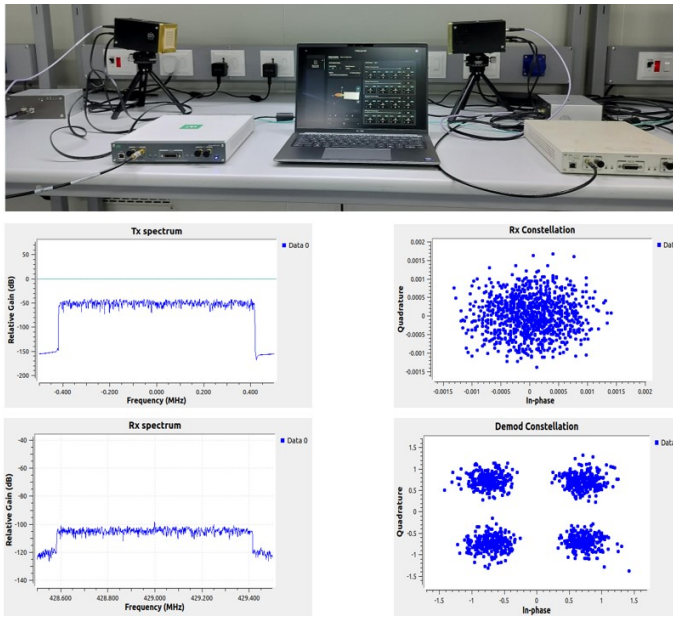

Fig. 14: Hardware setup at 0.75 metre and its simulation result

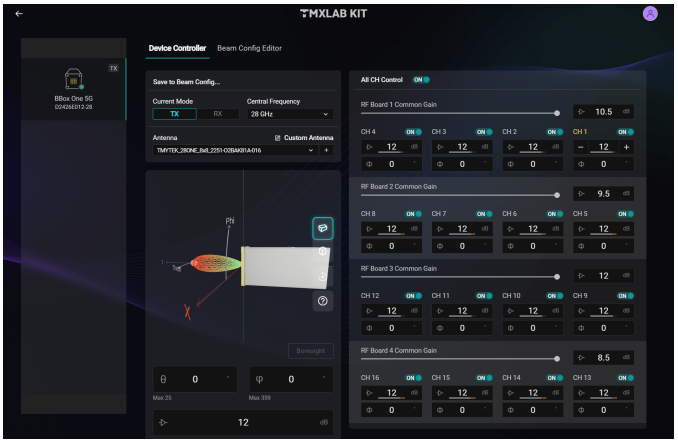

Fig. 15: TMYTEk Interface for BBox One 5G Transmitter [15]

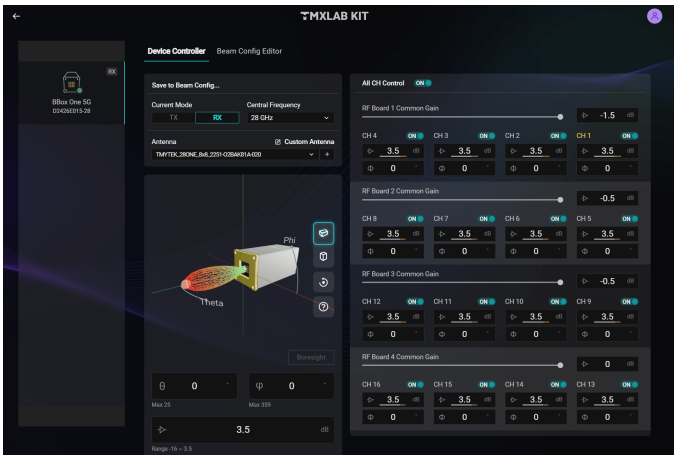

Fig. 16: TMYTEk Interface for BBox One 5G Reveiver [15]

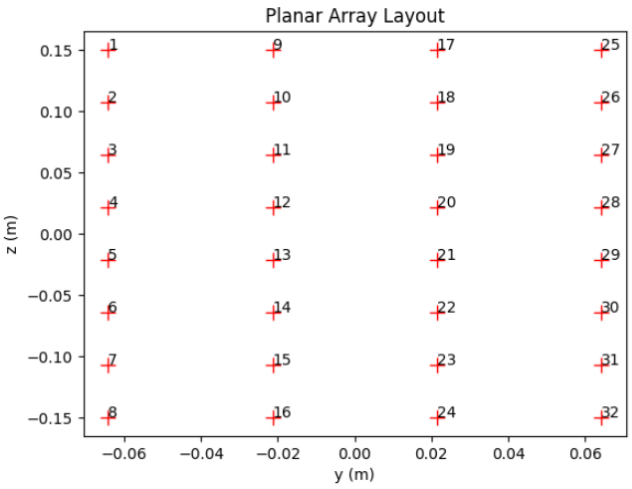

Fig. 17: Transmitter antenna array

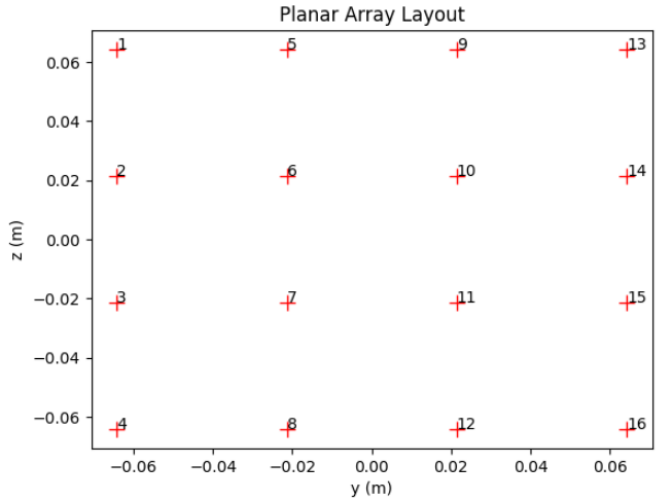

Fig. 18: Receiver antenna array

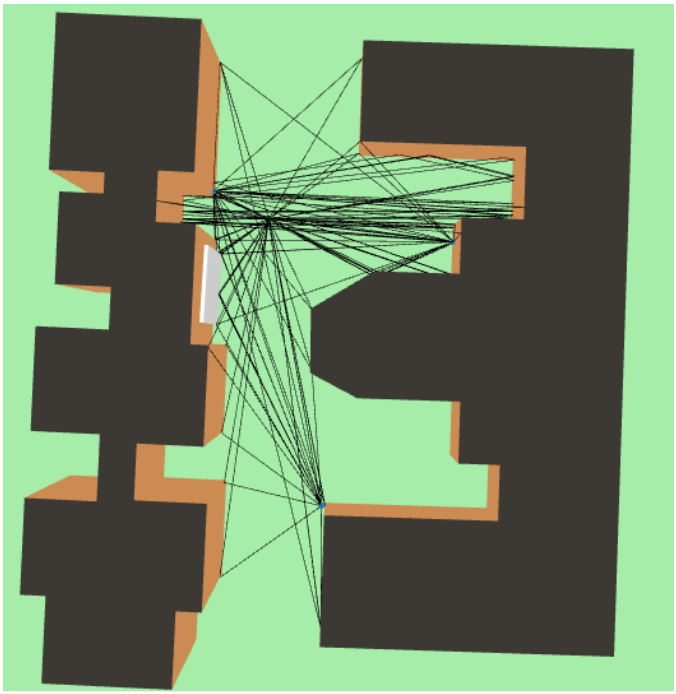

Fig. 19: Receiver at (-8,15), ECE Dept., IISc

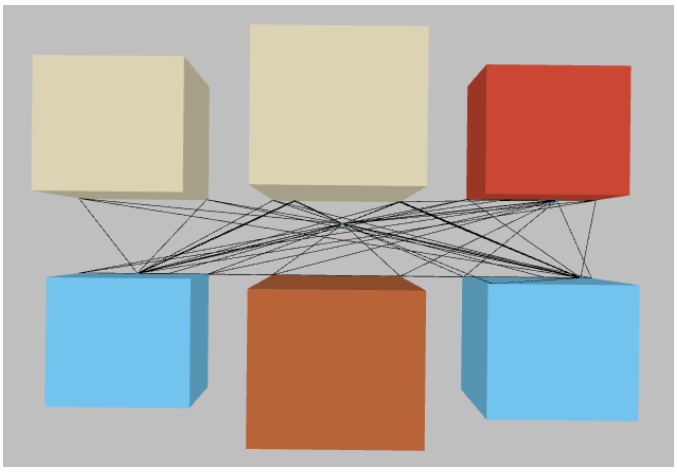

Fig. 20: Scene 2 (Simple street canyon)

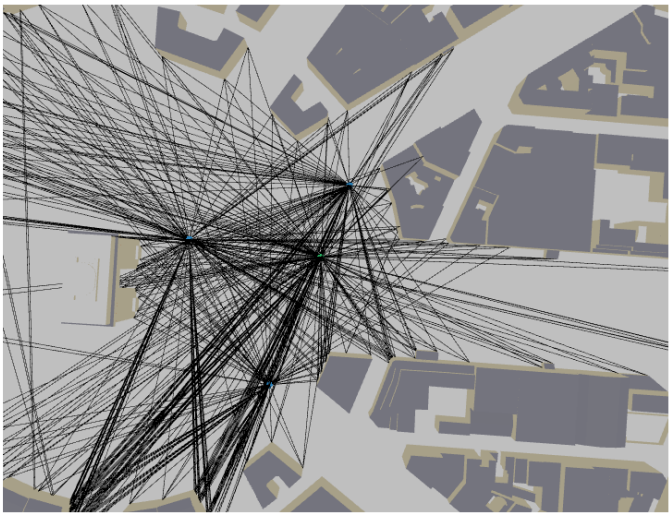

Fig. 21: Scene 3 (Etiole)

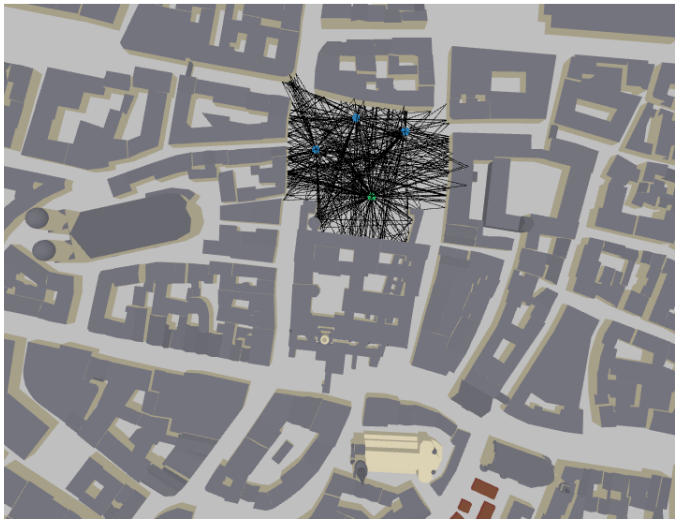

Fig. 22: Scene 3 (Munich)